View metadata, citation and similar papers at core.ac.uk

brought to you by CORE

ELSEVIER

International Journal of Minerals, Metallurgy and Materials
Volume 16, Number 1, February 2009, Page 43

Materials

Corrosion behavior of tempered dual-phase steel embedded in concrete

Oğuzhan Keleştemur[1)], *Mustafa Aksoy*[2)], *and Servet Yıldız*[1)]

1) Department of Construction Education, Firat University, Elazig 23119, Turkey

2) Department of Metallurgy and Materials Engineering, Firat University, Elazig 23119, Turkey

(Received 2008-02-20)

Abstract: Dual-phase (DP) steels with different martensite contents were obtained by appropriate heat treatment of an SAE1010 structural carbon steel, which was cheap and widely used in the construction industry. The corrosion behavior of DP steels in concrete was investigated under various tempering conditions. Intercritical annealing heat treatment was applied to the reinforcing steel to obtain DP steels with different contents of martensite. These DP steels were tempered at 200, 300, and 400°C for 45 min and then cooled to room temperature. Corrosion experiments were conducted in two stages. In the first stage, the corrosion potential of DP steels embedded in concrete was measured every day for a period of 30 d based on the ASTM C 876 standard. In the second stage, the anodic and cathodic polarization values of these steels were obtained and subsequently the corrosion currents were determined with the aid of cathodic polarization curves. It was observed that the amount of second phase had a definite effect on the corrosion behavior of the DP steel embedded in concrete. As a result of this study, it is found that the corrosion rate of the DP steel increases with an increase in the amount of martensite.

Key words: dual-phase steel; corrosion; tempering treatment; martensite; concrete

[*This work was financially supported by the Scientific Research Projects Management Council of the Firat University (No.2005/1119).*]

1. Introduction

Reinforced concrete is the most commonly used construction material all over the word [1]. The use of reinforced concrete structures is based on the principle that concrete is an ideal environment for steel. The high alkalinity of concrete causes the formation of a saturated hydrated iron oxide passivating film on reinforcing steel, which provides good protection against corrosion. However, depassivation may be induced by carbonation of the cover concrete or by the presence of chloride salts, thus initiating expansive corrosion of the steel, causing eventual damage to the surrounding concrete [2]. Concrete structures, bridges, buildings, sanitary and water facilities, and other reinforced concrete structures get severely damaged due to corrosion of the reinforcing steel. The resultant cracking and spalling of the concrete costs billions of dollars each year. The estimated corrosion damage of a bridge deck and support structures in USA is in the range of $170 and $550 million. It has been estimated that the replacement cost of concrete structures can be substantially higher [3]. In addition, due to the economic losses incurred, public safety is also affected. Losses of life associated with the collapse of bridges and structures are examples.

Several approaches were taken to obtain durable reinforced concrete structures. One approach is to improve the quality of plain concrete with the use of mineral admixtures such as silica fume, fly ash, and slag, to lower the permeability of the material, thus decreasing the ingress of deleterious substances and delaying depassivation of the steel [4-8]. An alternative and complementary approach is to improve the durability of the reinforcing steel. Epoxy coated and galvanized reinforcing steels have been marketed to alleviate the problems of corrosion of steel in concrete structures, but recent studies have shown that these treated bars only delay the initiation of corrosion [9-10].

Developed in the 1970s, dual-phase steels are identified as a class of high-strength low-alloy (HSLA)

Corresponding author: Oğuzhan Keleştemur, **E-mail:** okelestemur@firat.edu.tr

Also available online at www.sciencedirect.com

© 2009 University of Science and Technology Beijing. All rights reserved.

steels designated by a composite microstructure constituted by hard martensite particles dispersed in the soft ferrite matrix, where the soft ferrite matrix ensures high formability and the hard martensite provides the strengthening effects [11-14]. In addition to the high tensile strength, dual-phase (DP) steels are characterized by continuous yielding behavior, low yield stress, favorable yield strength to tensile strength ratio (~0.5), and a high level of uniform and total elongation value with a high work hardening coefficient. The combinations of all these properties make them attractive for application as very good quality sheet materials for the automotive industry [11-13, 15-17]. The unique combination of mechanical properties has led the researchers to explore the suitability of DP steels for structural and constructional purposes through replacement of pearlite wires, rods, and bars [17-21]. Besides a very good combination of mechanical properties, a priori knowledge about the corrosion behavior of DP steels is essential for assessing the true potential of DP steels in such applications [22]. Investigations in this direction though extremely limited, Jha *et al*. [19], Thomas [18], and Zhang *et al*. [23] have observed very good corrosion resistance properties in the DP microstructure. Trejo *et al*. [24] have also observed that DP steel has better corrosion resistance than the standard billet reinforcement in concrete.

Nevertheless, it was possible to find different approaches in the open literatures. For example, Sarkar *et al*. [22] tried to enhance the martensite content, to improve the mechanical properties of DP steels. However, results of this study showed worse corrosion behavior of DP steel in 3.5% NaCl solution. Kelestemur and Yildiz [25] studied the effect of the microstructure on the corrosion behavior of DP steels embedded in concrete. It was revealed that the corrosion rate of DP steels embedded in concrete had increased with an increase in the amount of martensite. The studies performed to determine the corrosion behavior of DP steels had not clarified the subject enough. Therefore, further studies on the corrosion behavior of DP steels, especially in concrete are needed for the effective use of these steels in the construction industry.

In this study, DP steels with different martensite contents were obtained by appropriate heat treatment of a SAE1010 structural carbon steel, which was cheap and used in a wide range in the construction industry, and the corrosion behavior of the DP steels in concrete was investigated at various tempering temperatures.

2. Experimental

2.1. Material and heat treatment

As an electrode, the SAE1010 steel bar produced by the Ereğli Iron and Steel Factories in Turkey, which is a fundamental construction material of the construction industry, was selected for the present study. The as-received material was in the form of a 12 mm-diameter hot-rolled bar with a ferritic-pearlitic structure. The chemical composition (wt%) of SAE1010 is C 0.176, Si 0.231, Mn 0.557, P 0.011, S 0.027, and Fe balanced.

The critical temperatures of the steel were determined by microscopic examination of the heat-treated specimens. Starting at 680°C, the specimens were heat treated in a neutral salt bath for environmental protection, and then quenched in a mixture of ice and water. The procedure was repeated at 10°C intervals. From the microscopic examinations, 730 and 840°C were found to be sufficiently close to the A_1 and A_3 (critical temperatures of the iron-carbon equilibrium diagram of steel) temperatures, respectively. However, at temperatures above 840°C, it was not possible to effectively transform austenite to martensite, due to the low carbon content of austenite, which impaired its hardenability. The specimens were heat treated at 730°C to increase the carbon content in the austenite phase.

Small specimens, 15 mm in length, were cut out from the as-received material for metallographic examinations. Corrosion specimens, 110 mm in length, were also cut out from the as-received material. All specimens were heat treated for 20, 40, and 60 min in the intercritical range (730°C) and quenched in a mixture of ice and water. The duration of austenization treatment was varied to obtain different martensite volume fractions (MHO). After quenching, all the specimens were tempered at 200, 300, and 400°C for 45 min, and then cooled to room temperature. In order to distinguish the specimens subjected to varied heat treatment schedules, they were identified with code numbers, as described in Table 1.

All the heat treatment cycles were carried out in a neutral salt bath whose temperature was controlled at ± 1°C for atmospheric environmental protection.

The microstructure of the specimens was observed under a light microscope following the usual metallographic polishing and etching with 2% nital solution. The grain size and volume fraction of the phase constituents were determined by the method given in ASTM E112 [26].

Table 1. Heat treatment schedules for achieving dual-phase microstructure

Specimen code	Temperature and duration for austenization treatment	Temperature and duration for tempering treatment
C	—	—
D20	730°C / 20 min	—
D22	730°C / 20 min	200°C / 45 min
D23	730°C / 20 min	300°C / 45 min
D24	730°C / 20 min	400°C / 45 min
D40	730°C / 40 min	—
D42	730°C / 40 min	200°C / 45 min
D43	730°C / 40 min	300°C / 45 min
D44	730°C / 40 min	400°C / 45 min
D60	730°C / 60 min	—
D62	730°C / 60 min	200°C / 45 min
D63	730°C / 60 min	300°C / 45 min
D64	730°C / 60 min	400°C / 45 min

2.2. Corrosion tests

A total of 65 concrete blocks were prepared to investigate the corrosion behavior of the DP steel produced from the reinforcing steel bar. Steel samples embedded in 100 mm×100 mm×200 mm concrete blocks were evaluated for corrosion behavior.

In the scope of the study, ASTM C 150 Type I Portland cement was used in order to prepare all the concrete samples included in the experiments. Chemical composition (wt%) of this cement is SiO_2 22.05, Al_2O_3 5.40, Fe_2O_3 3.18, CaO 63.07, MgO 2.21, SO_3 2.20, Cl^- 0.009, LOI 1.29, and unknown 1.80

The cement used in the concrete mixture had a density of 3100 kg/m^3. Tap water was used as mix water when preparing the concrete blocks. NaCl of 3.5% was added into the mix water of the concrete mortar for creating a corrosive environment. The concrete mixture had a water-to-cement ratio of 0.55 and a wet unit weight of 2237 kg/m^3.

The mixture proportion of concrete blocks in compliance with ACI 211.1 [27] is presented in Table 2.

Table 2. Mixture proportion of concrete blocks **kg·m^{-3}**

Cement	Water	Gravel (4-8 mm)	Sand (0-4 mm)	NaCl
400	220	560	1043	6.6

Corrosion experiments were conducted in two stages. In the first stage, the corrosion potential of steels embedded in concrete was measured every day for a period of 30 d in accordance with ASTM C-876 method [28]. In the second stage, the anodic and cathodic polarization values of steel embedded in concrete were obtained and then the corrosion currents were determined with the aid of cathodic polarization curves.

120 pieces of DP steel bars were machined to 11 mm diameter and 90 mm length to remove the decarburized layer and the sample surfaces were polished with 1200 mesh sandpaper. The polished surfaces were cleaned with ethyl alcohol. Surface areas of 10 cm^2 were left open at the tips of the electrodes. These would be embedded in concrete. Screw threads were machined at the other end of steel electrodes and cables were connected to these ends to make measurements easily during the experiment. The remaining sections of the electrodes were protected against external effects by initially covering them with epoxy resin and then with polyethylene wrap. Subsequently the electrodes were placed in 100 mm×100 mm×200 mm concrete blocks. 10 pieces of reinforcing steel bars in the as-received normal condition (*i.e.*, as used in construction practice) were also placed in similar forms in order to carry out corrosion experiments.

Experimental setup used for the application of Galvanostatic method is shown schematically in Fig. 1.

Black areas on the electrodes displayed in Fig. 1 indicate the areas kept under protection. In this circuit, the electrode that connected to the positive terminal is the anode and the electrode that connected to the negative terminal of the DC power source is the cathode. The DC power source is applied to the system and the application detail is given in elsewhere [12].

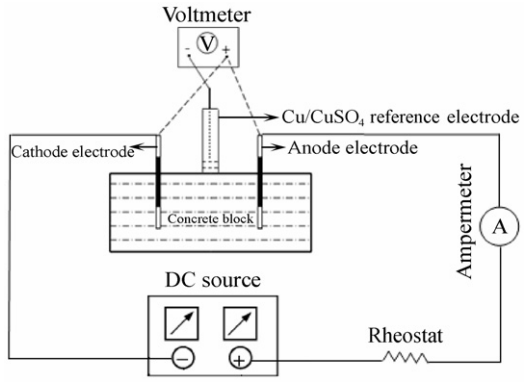

Fig. 1. Schematic representation of the polarization measurement using Galvanostatic method.

3. Results and discussion

3.1. Microstructure

The microstructure of the as-received specimen (C) shown in Fig. 2 reveals that the structure consists of uniformly distributed pearlite (dark grains) colonies in an equiaxed ferrite matrix.

The microstructures of DP steels developed by heat treatment for 20, 40, and 60 min at 730°C, and then quenched in a mixture of ice and water are shown in Fig. 3. It is observed that heat treatment of the specimen C directly to the intercritical temperature results in the development of a martensite network surrounding the ferrite grains. Such a morphological distribution of martensite is commonly termed as a ring, chain or a continuous network of martensite [22]. Initially, the microstructure of the DP specimens has ferrite and pearlite. When annealed in the (α+γ) region, austenite grains are nucleated at the carbide/ferrite interfaces, which transform to martensite after quenching. Ferrite grains appear unchanged from these observations in the as-received materials. The ferrite phase does not experience any structural change from the austenite-plus-ferrite region after quenching. On the other hand, it is observed on these micrographs that the volume fraction of the martensite phase increases with an increase in the duration of austenization. A similar relationship has also been reported by other researchers [20-25, 29-32]

The changes in the volume fraction and grain size of the phases are given in Table 3.

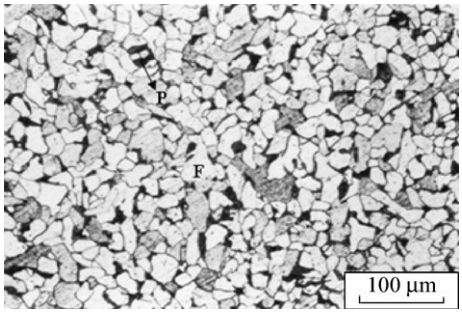

Fig. 2. Ferrite-pearlite structures being processed to produce dual-phase steel.

The increase in the volume fraction of martensite depends on the increase in austenization duration, which results in increasing the amount of austenite [20, 33]. As seen in Table 3, the ferrite grain size decreases, whereas, the martensite grain size increases to some extent with increasing austenization duration. As the austenite occurs first with the transformation of pearlite grains, the austenite grains grow, while the ferrite grains decrease due to the progress of the transformation in the ferrite grains. The average grain size of the phases in the microstructure decreases due to the decrease in ferrite grain size.

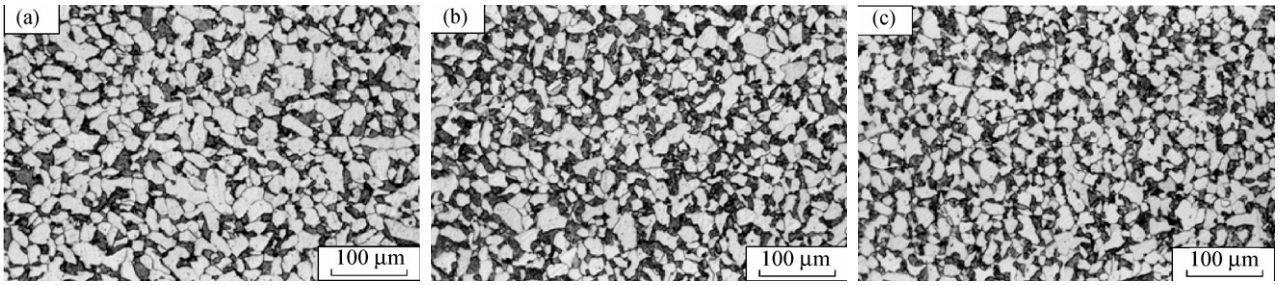

Fig. 3. Microstructures of DP steels: (a) D20; (b) D40; (c) D60.

Table 3. Metallographic data

Specimen	MHO / %	Ferrite grain size / μm	Martensite grain size / μm	Average grain size / μm
C	13.71*	44.61	18.69**	38.43
D20	22.68	43.99	21.37	36.03
D40	28.06	40.12	21.28	31.63
D60	30.58	39.3	22.74	30.3

Note: * pearlite volume fraction, ** pearlite grain size

3.2. Corrosion behavior

The corrosion potential of steels embedded in concrete was measured daily for a period of 30 d, in accordance with the ASTM C-876 standard. A saturated copper/copper sulfate (CSE) electrode was used as the reference electrode, and a high impedance voltmeter was used as the measurement device for the corrosion potential measurement. Changes in corrosion potentials with time were indicated as graphics in order to determine whether the steel was in an active or passive state.

The results obtained from corrosion potential measurements of the steels embedded in concrete samples are indicated in Figs. 4-7.

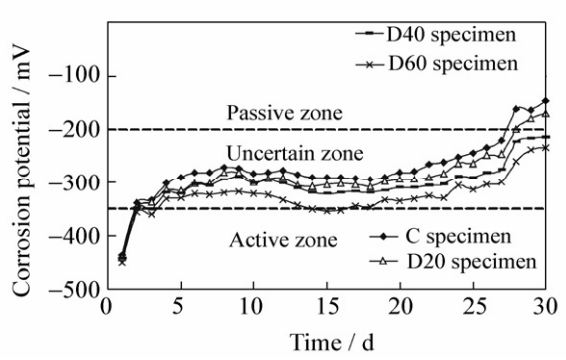

Fig. 4. Change in corrosion potential on the specimens C, D20, D40, and D60.

Recommendations on the evaluation of the potential measurement results in the ASTM C-876 experiment method are stated in Table 4.

As seen in Fig. 4, the corrosion rate is higher in all DP steels of any type compared to C steel. Some amount of increase in corrosion rate depends on the rise in the amount of martensite. Indeed, the specimen C became more passive compared to the DP specimens and together with the specimen D20 have reached the passive zone, in terms of corrosion, at the 27th day. The specimens D40 and D60 remain in the uncertain zone even at the 30th day. It indicates that the specimen D20 has the highest corrosion resistance among the DP specimens, which is quenched but not tempered. The specimen D60 exhibited the lowest passivation rate among the DP specimens, which is not subjected to tempering heat treatment.

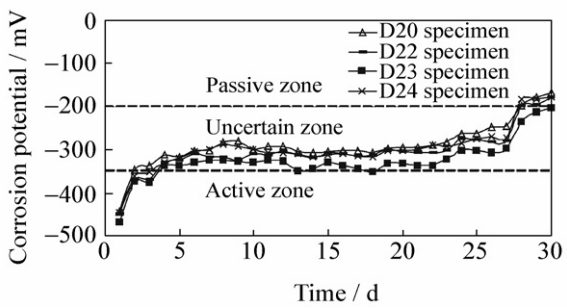

Fig. 5. Change in corrosion potential on the specimens D20, D22, D23 and D24.

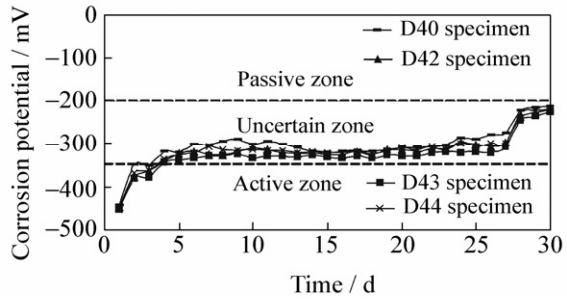

Fig. 6. Change in corrosion potential on the specimens D40, D42, D43 and D44.

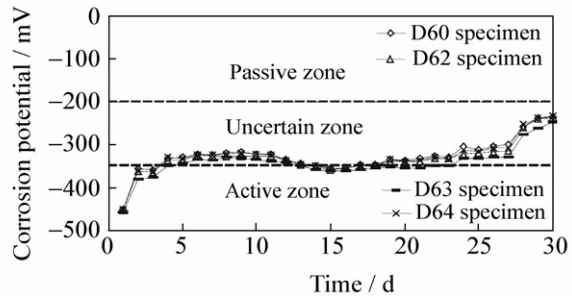

Fig. 7. Change in corrosion potential on the specimens D60, D62, D63 and D64.

Table 4. Estimation of corrosion probability as determined by half-cell potential test

Potential / mV *vs*. CSE	Probability of the presence of active corrosion
>–200	The probability for corrosion is very low
–200 - –350	Uncertain
<–350	The probability for corrosion is very high

As seen Figs. 5-7, tempering heat treatment, which is applied to DP steels, reduces the passivation rate of DP steels. In addition, the lowest passivation rate among the tempered DP steels occurs in the tempered specimens at 300°C. In this situation, it is stated that DP steels that have been subjected to tempering heat treatment have a lower corrosion resistance than DP steels that have not been subjected to tempering heat treatment.

From the results of corrosion potential by the ASTM C-876 standard, it is concluded that the reinforcing steel, with a microstructure of ferrite and pear-

lite, has a higher corrosion resistance than DP steels, and tempering heat treatment reduces the corrosion resistance of DP steels.

The corrosion potential provides qualitative and probably indicates on the corrosion of steel embedded in concrete. Quantitative and reliable information on the corrosion of steel embedded in concrete can be obtained by measuring the resistance or current density.

Results of corrosion polarization studies on the developed materials with respect to a copper sulfate electrode are shown in Table 5. The data of corrosion current density (I_{corr}) shown in Table 5 have been derived from the experimentally obtained cathodic polarization curves using Tafel's linear extrapolation method.

Table 5. Corrosion current density values of the investigated steels

Specimen	MHO / %	I_{corr} / (μA·cm^{-2})
C	13.71*	0.1437
D20	22.68	0.1629
D22		0.3049
D23		0.3413
D24		0.2847
D40	28.06	0.2438
D42		0.2821
D43		0.3354
D44		0.3014
D60	30.58	0.2687
D62		0.3921
D63		0.4318
D64		0.3805

Note: * pearlite volume fraction

As is clearly seen in Table 5, the corrosion rate is higher in all DP steels of any type compared with the reinforcing steel with a microstructure of ferrite and pearlite. In addition, the corrosion rate has been increased depending on the increase in the volume fraction of martensite. The corrosion current density values obtained from the cathodic polarization curves using Tafel's linear extrapolation method are naturally supporting the corrosion potential values. The changes in the volume fraction of martensite and corrosion rate depending on austenization duration are shown in Fig. 8.

In this situation, it can be said that the amount of the second phase has a definite effect on the corrosion behavior of the DP steel. The martensite phase will be the anode because the inner energy of ferrite phase, which exists in the DP microstructure, is lower than that in martensite phase. Therefore, the number of corrosion cell has increased with the increasing of martensite phase, and the corrosion rate has also increased. Besides, the average grain size of the DP microstructure has decreased with an increase in austenization duration, as seen in Table 3. This situation shows that the interfacial area between ferrite (cathode) and martensite (anode) has increased. This increase in the interfacial area causes an increase in the corrosion cell and the corrosion current at the same time.

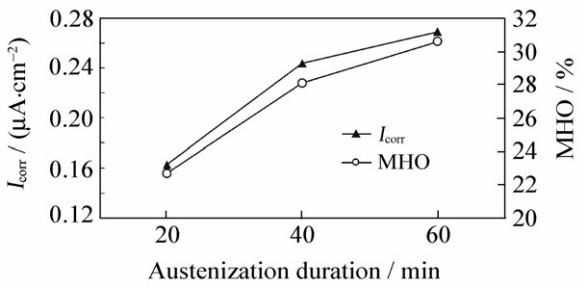

Fig. 8. Changes of MHO and I_{corr} with austenization duration.

The changes in the corrosion rate of DP steels depending on the tempering temperature are shown in Fig. 9.

As is clearly seen in Fig. 9, the corrosion rate of DP steels is increased by tempering heat treatment.

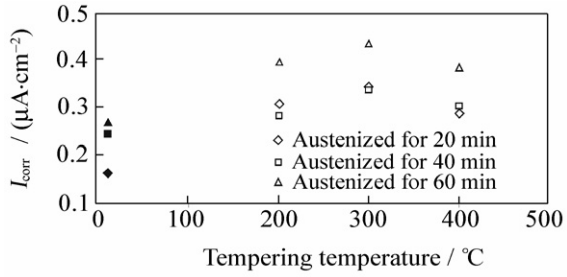

Fig. 9. Changes in the I_{corr} of specimens with tempering temperature.

There are two viewpoints with regard to the fact that tempering treatment affects DP steels having ferrite and martensite phases. The ferrite phase has a higher carbon content because it is melted at room temperature, due to rapid cooling from intercritical region. The carbon element in the ferrite phase precipitates as cementite (Fe_3C) due to the effect of tempering heat treatment. Therefore, new corrosion cells occur in the ferrite phase, as seen in Fig. 10.

The results of microstructure examination show that the tempering temperature at which a lot of cementite grains occur is 300°C. The effects of three various tempering temperatures on the cementite ratio in the ferrite phase are shown in Fig. 11. As seen in Fig. 11, the highest cementite ratio in the ferrite phase is in the specimen tempered at 300°C.

The martensite phase was also affected by the tempering treatment as similar to the ferrite phase. As tempering treatment up to 200°C, the stress was reduced and the phase of ε carbide occurred [34]. New corrosion cells occurred in the tempered martensite phase. Cementite phases occurred with an increase in tempering temperature and replaced ε carbide. However, the amount of cementite phase has decreased with an increase in temperature and the grains have grown spherically [34]. Therefore, the corrosion cells in the martensite phase have reduced due to an increase in tempering temperature.

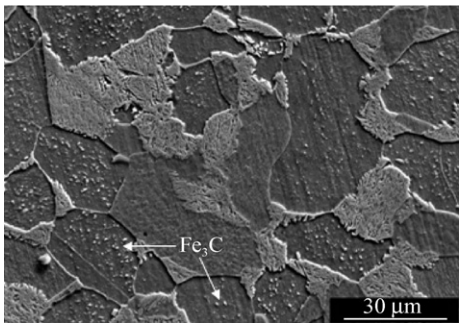

Fig. 10. SEM micrograph indicating the cementite grains.

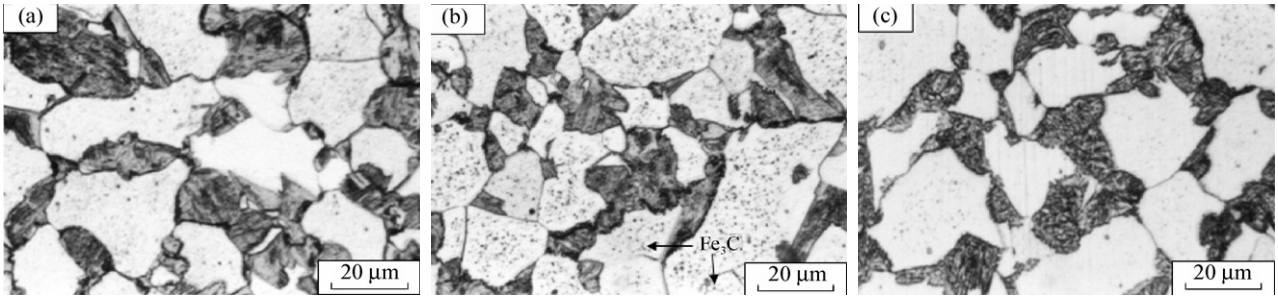

Fig. 11. Effect of tempering temperature on the cementite ratio in the ferrite phase: (a) D62; (b) D63; (c) D64.

It is understood from earlier explanations that the corrosion behavior of the DP steel has improved depending on the corrosion behavior of two phases. As a result of the experiments, it is seen that cementite grains in the ferrite phase are more effective for the corrosion behavior of DP steels. As seen in Fig. 9, the corrosion rate of specimens tempered at 300°C is higher, whereas, the corrosion rates of specimens tempered at 200 and 400°C, having approximately the same amount of cementite, have almost the same values.

4. Conclusions

On the basis of the experimental study that has been carried out and presented in this article, the following conclusions can be drawn.

(1) Dual-phase steel can be produced from reinforcing steel with austenization and quenching treatments in the (α+γ) region.

(2) The volume fraction and grain size of phases in the dual-phase microstructure have changed depending on austenization duration. The volume fraction of martensite has increased and the average grain size has reduced with an increase in austenization duration.

(3) The experiments conducted to determine the corrosion behavior of dual-phase steel in concrete show that the corrosion resistance of dual-phase steel is lower than that of reinforcing steel with a microstructure of ferrite and pearlite. The corrosion rate of dual-phase steel embedded in concrete increases depending on the increase in the volume fraction of martensite. In addition, the corrosion rate of the dual-phase steel increases with tempering heat treatment and the highest corrosion rate takes place in dual-phase steel tempered at 300°C .

(4) The corrosion behavior of dual-phase steel has changed while the corrosion rate of two phases changes. However, it is understood that cementite grains in the ferrite phase are more effective for the corrosion behavior of dual-phase steel.

References

[1] K.K. Sideris and A.E. Sava, Durability of mixtures containing calcium nitrite based corrosion inhibitor, *Cem. Concr. Compos.*, 27(2005), p.277.

[2] J.A. Gonzalez, A. Molina, E. Otero, and W. Lopez, On the mechanism of steel corrosion in concrete: the role oxygen diffusion, *Mag. Concr. Res.*, 42(1990), p.23.

[3] J.P. Broomfield, Strategic highway research programmer on corrosion of steel in concrete, *Bull. Electrochem.*, 11(1995), No.4, p.169.

[4] W.E. Ellis, E.H. Riggs, and W.B. Butler, Comparative results of utilization of fly ash, silica fume and GGBFS in reducing the chloride permeability of concrete, durability of concrete, [in] *Second International Conference*, Montreal, 1991, p.443.

[5] Rasheeduzzafar, S.S. Al-Saadoun, and A.S. Al-Gahtani, Reinforcement corrosion-resisting characteristics of silica-fume blended cement concrete, *ACI Mater. J.*, 89(1992), No.4, p.337.

[6] F. Massazza and G. Oberti, Durability of pozzolonic cements and Italian experience in mass concrete, durability of concrete, [in] *Second International Conference*, Mont-

real, 1991, p.1259.

[7] A.K. Parande, B.R. Babu, M.A. Karthik, K.K.D Kumaar, and N. Palaniswamy, Study on strength and corrosion performance for steel embedded in metakaolin blended concrete/mortar, *Constr. Build. Mater.*, 22(2008), No.3, p.127.

[8] K.M.A. Hossain and M. Lachemi, Corrosion resistance and chloride diffusivity of volcanic ash blended cement mortar, *Cem. Concr. Res.*, 34(2004), p.695.

[9] A. Sagues, R. Powers, and A. Zayed, Marine environment corrosion of epoxy-coated reinforcing steel, corrosion of reinforcement in concrete, [in] *Corrosion of Reinforcement in Concrete Structures*, SCI, 1990, p.539.

[10] Rasheeduzzafar, F.H. Dakhil, M.A. Bader, and M.M. Khan, Performance of corrosion resisting steels in chloride bearing concrete, *ACI Mater. J.*, 89(1992), No.5, p.439.

[11] D.T. Llewellyn, Copper in steels, *Ironmaking Steelmaking*, 22(1995), p.25.

[12] D.T. Llewellyn and D.J. Hills, Dual phase steels, *Ironmaking Steelmaking*, 23(1996), p. 471.

[13] R.G. Davies and C.L. Magee, Physical metallurgy of automotive high strength steels, [in] *Structure and Properties of Dual-Phase Steels*, New York, 1979, p.1.

[14] A.H. Nakagawa and G. Thomas, Metallurgical transactions, *Phys. Metall. Mater. Sci. A*, 16(1985), p.831.

[15] G.R Speich and R.L. Miller, Mechanical properties of ferrite-martensite steels, [in] *Structure and Properties of Dual-Phase Steels*, New York, 1979, p.1.

[16] O. Keleştemur, *An Investigation on the Usability and Corrosion Resistance of the Dual-Phase Steel in the Rein-forced Concrete Structures* [Dissertation], Firat University, Elazig, Turkey, 2008.

[17] G.R. Speich, Physical metallurgy of dual-phase steels, Fundamentals of dual-phase steel, [in] *Steels in Fundamentals of Dual Phase Steels*. New York: The American Institute of Mining, Metallurgical, and Petroleum Engineers, 1981, p.1.

[18] G. Thomas, Improved properties of HSLA and dual-phase steels by controlled rolling and direct quenching, [in] *Physical Metallurgy of Direct Quenched Steels*, TMS, 1993, p.265.

[19] B.K. Jha, R. Avtar, and D.V. Sagar, Structure-property correlation in low carbon low alloy high strength wire rods/wires containing retained austenite, *Trans. Indian Inst. Met.*, 49(1996), No.3, p.133.

[20] M. Aksoy and A. Esin, Improving the mechanical properties of structural carbon steel by dual-phase heat treatment, *J. Mater. Eng.*, 10(1988), p.281.

[21] K.S. Park, K.T. Park, D.L. Lee, and C.S. Lee, Effect of heat treatment path on the cold formability of drawn dual-phase steels, *Mater. Sci. Eng. A*, 449(2007), p.1135.

[22] P.P. Sarkar, P. Kumar, K.M. Mana, and P.C. Chakraborti, Microstructural influence on the electrochemical corrosion behavior of dual-phase steels in 3.5% NaCl solution, *Mater. Lett.*, 59(2005), p.2488.

[23] C. Zhang, D. Cai, B. Liao, T. Zhao, and Y. Fan, A study on the dual-phase treatment of weathering steel 09CuPCrNi, *Mater. Lett.*, 58(2004), p.1524.

[24] D. Trejo, P. Monteiro, G. Thomas, and X. Wang, Mechanical properties and corrosion susceptibility of dual-phase steel in concrete, *Cem. Concr. Res.*, 24(1994), p.1245.

[25] O. Kelestemur and S. Yildiz, Effect of various dual-phase heat treatments on the corrosion behavior of reinforcing steel used in the reinforced concrete structures, *Constr. Build. Mater.,* 23(2009), p.78.

[26] ASTM E112-96, *Standard Test Methods for Determining Average Grain Size*, ASTM International, 2004.

[27] ACI 211.1, *Standard Practice for Selecting Proportions for Normal, Heavyweight and Mass Concrete*, American Concrete Institute, 1991.

[28] ASTM C876-91, *Standard Test Method for Half-Cell Potentials of Uncoated Reinforcing Steel in Concrete*, Vol. 4.02. Annual Book of ASTM Standards, Philadelphia, USA, 1991.

[29] E. Ahmed, T. Manzoor, A.K. Liaqat, and J.I. Akhter, Effect of microvoid formation on the tensile properties of dual-phase steel, *J. Mater. Eng. Perform.*, 9(2000), p.306.

[30] E. Ahmed and R. Priestner, Effect of rolling in the intercritical region on the tensile properties of dual-phase steel, *J. Mater. Eng. Perform.*, 7(1998), p.772.

[31] M. Sarwar and R. Priestner, Influence of ferrite-martensite microstructural morphology on tensile properties of dual-phase steel, *J. Mater. Sci.*, 31(1996), p.2091.

[32] M. Erdogan, S. Tekeli, O. Pamuk, and A. Erkan, Surface carburized AISI8620 steel with dual-phase core microstructure, *Mater. Sci. Technol.*, 18(2002), p.840.

[33] J.M. Rigsbee and P.J. Vanderarend, Laboratory studies of microstructures and structure-property relationships in dual-phase HSLA steels, [in] *TMS-AIME Fall Meeting*, Chicago, 1977, p.56.

[34] K.E. Thelning, *Steel and Its Heat Treatment*, Butterworth Press, London, 1984, p.704.